HEFAT2010
7th International Conference on Heat Transfer, Fluid Mechanics and Thermodynamics
19-21 July 2010
Antalya, Turkey

A two-phase flow model for H_2 evolution in a membrane reactor cell

Farshad Abbasi *
*Author for correspondence
Mechanical Engineering Department, Islamic Azad University of Marivan, P.O.Box 394, Marivan, I.R.IRAN.

Hasan Rahimzadeh
Mechanical Engineering Department, Amirkabir University of Technology, Tehran, I.R.IRAN.

ABSTRACT

Membrane reactors are currently under extensive research and development. In this paper, a numerical study is presented on the hydrogen evolution and flow field in a membrane rector using a two-phase flow model. The model solves transport equations for both phases with an allowance to inter-phase mass and momentum exchange. The effects of current density, electrolyte flow rate and distance between electrodes on the gas release rate are investigated in a range of parameter and cell optimization. The finite volume discretization scheme is used to create a linearized system of equations that are solved by SIMPLE staggered grid solution technique for a rectangular channel. It is found that the gas void fraction increases towards to the top of the cell. Hydrogen generation significantly increases at higher electrolyte flow by reducing the residence time of bubbles over the electrode. The predicted results satisfactorily agree with data available in the literature.

INTRODUCTION

The integration of chemical conversion and separation into a single processing step offers opportunities towards process intensification. The later is one of the major forms of sustainable technology development. Membrane reactors are a particular form of the integration of conversion and reaction. A large variety of combinations can be realized in membrane reactors as one easily conceives from the large variety of different reactions as well as membrane separation processes.

Membrane reactors are heavily investigated in the academic and industrial domain. However, only few industrially relevant and realized examples are known in literature. Vogt [1] performed a variety of experiments to observe the gas release behavior on an electrolysis cell and showed that at the low current densities, evolved gas leaved the surface mainly by molecular diffusion. At higher current densities, gas bubbles were nucleated at several locations on the electrode and grown with dissolved gas in the electrolyte. The relation between the transport of electrochemical evolved Hydrogen and Chlorine, from the electrode surface into the bulk of solution by convective diffusion and by gas bubbles, was experimentally obtained at a temperature of 25°C by L. Muller et al [2]. They found that, that at high current densities (in the range of technical current densities) the chlorine as well as the hydrogen evolved leave the electrode surface partially by convective diffusion. Reigel et al [3] identified two flow regimes in an electrolyzer cell depending on the current density. At low current densities, gas evolution became small and two-phase flow region confined in a very small region adjacent to the electrode, however, at higher current densities, a back flow leading occurred by the increase of electrolyte resistance.

In a range of current density Fukunaka et al [4] found that the mass transfer coefficient increased at higher current densities. This trend was attributed to transition to turbulence at higher current densities. Boissanneau and Byrne [5] investigated velocity field in an electrochemical cell with vertical electrodes for hydrogen production. Advanced measurement systems such as Laser Doppler Anemometry (LDA) and Particle Image Velocitymetry (PIV) were employed to determine flow field. They showed that even though the flow was laminar in terms of relevant Reynolds number range considered, bubbles caused local turbulence by causing velocity fluctuations due to the interactions with continuous phase. Therefore, both laminar and turbulent regimes exist in the system.

The bubbles growth and accumulation on the electrodes significantly affect the conductivity of the electrolyte mainly reducing the active area. Hine and Murakami [6] measured current density under the forced and natural convection states. They found that the current density significantly decreased along the electrode in a bottom-up direction due to the bubble enrichment.

Dahlkild [7] applied a mixture of two-phase flow model for electrolysis process and modified the model by applying a boundary layer analysis. The numerical results of Dahlkild showed that the non-uniform bubble distributions along the electrodes would result in a non-uniform current density distribution.

Mat et al [8] developed a two-fluid mathematical model for hydrogen production in a natural flow electrochemical system and found that model successfully captures the main characteristics of the electrolysis process. In the recent study of

Sherman et al [9] a two-fluid mathematical model coupled with population balance approach is used to numerical simulation of bubbly flow in a vertical isothermal channel. A numerical simulation of bubbly flow in the turbulent boundary layer of a horizontal parallel plate electrochemical reactor is investigated numerically by Thomas Nierhaus et al [10].

The main objective of this study is to investigate the hydrogen gas release in an electrolysis process from two-phase flow point of view and to study the effects of various parameters on the system performance.

NOMENCLATURE

C_d	[-]	drag coefficient,
D	$[m^2/s]$	diffusion coefficient,
d_b	$[m]$	bubble diameter,
F	$[C/mol]$	Faraday constant,
F_r	$[kg/m^2s^2]$	volumetric inter-fluid friction,
i	$[A/m^2]$	current density,
p	$[pa]$	static pressure,
R	$[J/mol^0K]$	universal gas constant,
Re	[-]	Reynolds number
T	$[^0K]$	temperature,
u	$[m/s]$	x-velocity vector,
v	$[m/s]$	y-velocity vector,
F_b	$[kg/m^2s^2]$	buoyancy forces,
g	$[m/s^2]$	gravity vector,
H	$[m]$	height of electrode,
W	$[m]$	width of channel,
A	$[1/m]$	interfacial area per unit volume,
N	$[1/m^3]$	number of bubbles per unit volume,
Greek letters		
α	[-]	void fraction
ρ	$[kg/m^3]$	density,
η	$[Volt]$	anodic over potential,
ϕ	$[Volt]$	electric potential,
μ	$[N.s/m^2]$	viscosity,
Subscripts		
b	-	bubble
g	-	gas phase
l	-	liquid phase
nb	-	neighbor
P	-	unknown node
W	-	west of node P
E	-	east of node P
N	-	north of node P
S	-	south of node P

MATHEMATICAL MODEL

In the membrane reactor cell, the anode and cathode are separated by means of a Cation-Exchange Membrane (CEM) (see Fig. 1). In this case, a saturated NaCl solution is passed through the anolyte compartment and Cl_2 gas is produced at the anode. Sodium ions (Na^+) migrate through the CEM into the catholyte compartment where they combine with hydroxide ions (OH^-) produced in the cathode to form hydroxide and H_2 gas. The reactions proceed according to the following relations:

AT THE CATHODE

$$2H_2O + 2e^- \rightarrow 2OH^- + H_2, \qquad 2Na^+ + 2OH^- \rightarrow 2NaOH, \tag{1}$$

AT THE ANODE

$$2NaCl \rightarrow 2Na^+ + 2Cl^-, \qquad 2Cl^- \rightarrow Cl_2 + 2e^-, \tag{2}$$

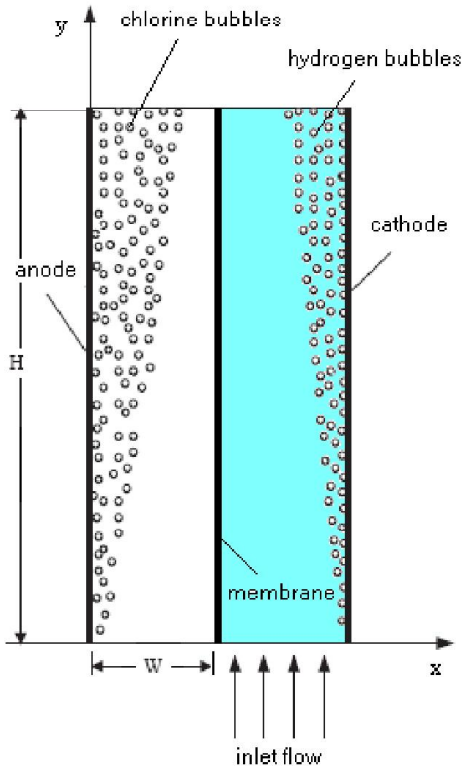

Fig. 1. Schematic sketch of a membrane reactor.

Since hydrogen evolution is the primary purpose of the electrolysis, only the region between the cathode and membrane is considered in this study. Configuration and dimensions of the system are considered as the mirror of the experimental study of Jean St-Pierre et al [11].

The interest of the present study is limited to the electrochemical reaction and bubbly flow, therefore, in the two-fluid mathematical model here, the liquid is treated as the continuous phase and the vapor bubbles the dispersed phase. Two sets of conservation equations governing the balance of mass and momentum of each phase are solved. Since the macroscopic fields of one phase are not independent of the other phase, the interaction terms which couple the transport of

mass and momentum across the interfaces appear in the field equations as follow:

MASS CONSERVATION

$$\frac{\partial}{\partial t}(\alpha_i \rho_i)+\frac{\partial}{\partial x}(\rho_i \alpha_i u_i)+\frac{\partial}{\partial y}(\rho_i \alpha_i v_i)=M_{i-\text{int}}, \tag{3}$$

where subscript, i represents the phases and takes the value of l, g in this problem. The term in the right hand of this equation represents the diffusion of one phase to the other phase.

X-MOMENTUM

$$\begin{aligned}&\frac{\partial}{\partial t}(\rho_i \alpha_i u_i)+\frac{\partial}{\partial x}(\rho_i \alpha_i u_i^2)+\frac{\partial}{\partial y}(\rho_i \alpha_i u_i v_i)=\\&-\frac{\partial}{\partial x}(p\alpha_i)+F_r(u_j-u_i)+\frac{\partial}{\partial x}(\alpha_i \mu_{eff_i}\frac{\partial u_i}{\partial x})+\\&\frac{\partial}{\partial y}(\alpha_i \mu_{eff_i}\frac{\partial u_i}{\partial y}),\end{aligned} \tag{4}$$

Y-MOMENTUM

$$\begin{aligned}&\frac{\partial}{\partial t}(\rho_i \alpha_i v_i)+\frac{\partial}{\partial x}(\rho_i \alpha_i u_i v_i)+\frac{\partial}{\partial y}(\rho_i \alpha_i v_i^2)=\\&-\frac{\partial}{\partial y}(p\alpha_i)+F_r(v_j-v_i)+\frac{\partial}{\partial x}(\alpha_i \mu_{eff_i}\frac{\partial v_i}{\partial x})+\\&\frac{\partial}{\partial y}(\alpha_i \mu_{eff_i}\frac{\partial v_i}{\partial y})+F_b,\end{aligned} \tag{5}$$

F_r in both momentum equations is interface friction term and represents momentum exchange between the phases per unit volume and $F_b=\rho g$ is the buoyancy force where g being the gravity vector.

AUXILIARY EQUATIONS

Mass diffusion between the two phases at the gas–liquid interface, $M_{i-\text{int}}$ is calculated as [12]:

$$M_{i-\text{int}}=\frac{\partial}{\partial x}(\rho_i D_i\frac{\partial \alpha_i}{\partial x})+\frac{\partial}{\partial y}(\rho_i D_i\frac{\partial \alpha_i}{\partial y}), \tag{6}$$

where D_i represents diffusion coefficient of phase i and may be expressed as [8]:

$$D_i=\mu_{eff,i}, \tag{7}$$

where $\mu_{eff,i}$ is the effective viscosity of phase i.

Interface friction term, F_r in momentum equations can be expressed as:

$$F_r=\frac{1}{8}C_d A_{\text{lg}}\alpha_l\frac{\mu_l}{d_b}\text{Re}_b, \tag{8}$$

where C_d, A_{lg} represent the drag coefficient and interfacial area per unit volume, respectively. Assuming that bubbles have a spherical shape with a characteristic diameter of d_b, the drag coefficient is given by [13]:

$$C_d=\frac{24.0}{\text{Re}_b}(1+0.15\,\text{Re}_b^{0.687})+\frac{0.42}{(1+\frac{42500}{\text{Re}_b^{1.16}})}, \tag{9}$$

where Re_b is the Reynolds number based on the gas bubble diameter:

$$\text{Re}_b=\frac{\rho_l|U_l-U_g|d_b}{\mu_l}, \tag{10}$$

where $|U_l-U_g|$ is the slip velocity vector between the two phases.

The interfacial area concentration A_{lg} is related to the gas void fraction α_g and the bubble diameter d_b as follow [14]:

$$A_{\text{lg}}=\frac{6\alpha_g}{d_b}, \tag{11}$$

It is seen that bubble diameter, d_b is an important parameter determining interphase friction between two phases.

The normal component of departure gas phase velocity on the electrode surface can be calculated using Faraday's law. Assuming all hydrogen produced as a result of electrochemical reaction transform into the gaseous phase, the normal velocity component at the cathode (hydrogen producing electrode) can be expressed as [8]:

$$u_g=\frac{1}{2}\frac{RT}{P_{H_2}}\frac{i(y)}{F}, \tag{12}$$

where *T, R, P, F* are temperature (assumed to be constant in this study), universal gas constant, pressure of gaseous phase and Faraday constant, respectively. The multiplication of normal velocity with electrode surface area gives volumetric production of hydrogen gas. The factor $\frac{1}{2}$ represents the fact that two electrons must be transferred for the production of each hydrogen molecule. $i(y)$ is the current density at the electrode surface and is calculated as [8]:

$$i(y)=-i_0(1-\alpha_g)\exp(-\frac{F}{2RT}\eta), \tag{13}$$

where i_0 is the exchange current density, $(1-\alpha_g)$ represents reduction of the active electrode area due to the bubbles on the electrode. η represents the over potential calculated as:

$$\eta=-\phi, \tag{14}$$

where ϕ represents the electric potential being 3.3 Volt in this study.

NUMERICAL METHOD

The finite volume method is employed to discrete the governing equations. A staggered grid is adopted to obtain a compact stencil for pressure. On the staggered grids, the flow properties such as volume fraction, density and pressure are located at the center of the main control volume. The whole set of equations is solved by incorporating the SIMPLE algorithm

of Patankar and Spalding [15]. Because of the nonlinearity of the governing equations and the coupling of variables, iterative numerical procedures are conducted until the convergence is reached.

SENSITIVITY ANALYSIS: INFLUENCE OF GRID ARRANGEMENT

Prior to evaluating the models, the influence of grid density on the precision of numerical results was analyzed. Therefore, a two-dimensional computational domain was built and three different grid arrangements (10*80, 15*80, 20*80 uniform rectangular cells) were tested. It is found that there is no significant difference between the predicted results of the 15*80 and the 20*80 grid arrangements. Therefore it is confirmed that the 15*80 grid arrangement is adequate to the issue of the present study.

RESULTS AND DISCUSSIONS

The predicted results include the hydrogen gas void fraction and the effects of several processing parameters on the hydrogen evolution. The predicted gas void fraction profiles at three vertical sections in the system (H is the height of the electrode), compared with the experimental data's of Muller et al [2], are presented in Fig. 2. In this figure and subsequent figures $x=0mm$ corresponds to the location of the electrode (cathode) while $x=4mm$ is the membrane location. It is seen that, the predicted void fraction is the highest near the electrode, drops sharply within about 0.8 mm and then decreases gradually towards the membrane. The lateral void fraction distribution also increases from the bottom to the top of the electrode, due to the mixing and diffusion of the gas phase along the channel. The significant decrease along the lateral direction may be attributed to the forced convection. Although the void fraction is significantly higher towards the top of the channel, the rate of gas release decreases in this direction mainly due to a decrease in the current density as the void fraction increases. Our simulation is in a good agreement with the experimental results.

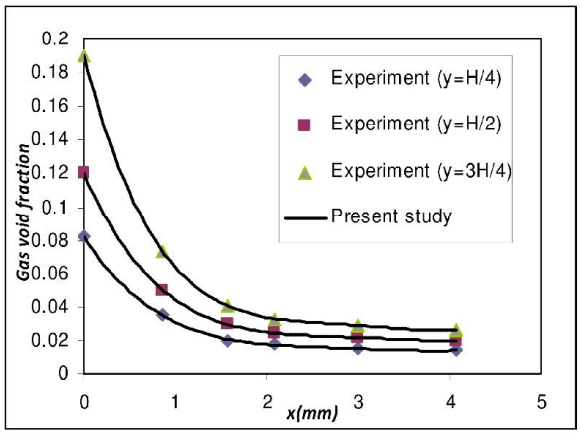

Fig. 2. Predicted gas void fraction distribution at three locations along the channel.

The effect of the electrolyte flow rate on the gas evolution at the mid-section of the electrode ($y=H/2$), is presented in Fig. 3. It is seen that, gas release increases with an increase in the electrolyte velocity. This trend is due to the decrease in the residence time of the gas bubbles on the electrode, resulting in an enhanced electrochemical reaction. At higher velocity, the gas motion is confined to a small region in the vicinity of the electrode. Due to the strong electrolyte flow the gas bubbles cannot diffuse in the lateral direction. On the other hand, at a lower velocity, the gas release rate significantly decreases due to the increased residence time of bubbles that attenuates the electrochemical reaction. At an intermediate velocity level the gas bubbles can penetrate far into the electrolyte due to molecular diffusion and mixing.

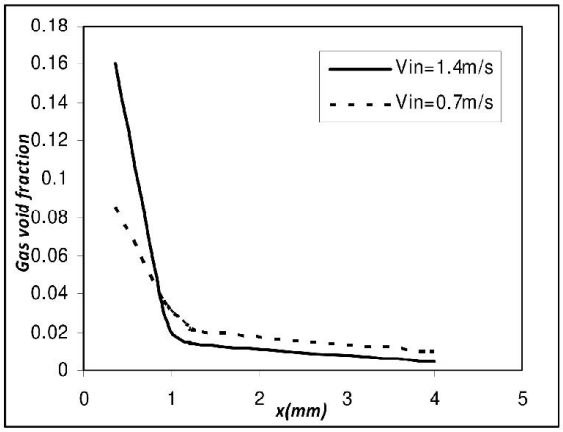

Fig. 3. Effect of the electrolyte flow rate on the gas release ($y=H/2$).

The effect of the current density on the gas release at the mid-section of the electrode ($y=H/2$) is shown in Fig. 4. It is seen that the gas release rate increases at higher current densities as expected. At higher current densities gas penetrates at lateral direction mainly because of the increase in lateral gas velocities. It is seen that the hydrogen release rate is not proportional to the increase in the current density. This is the result of accumulation of gas on the electrodes which adversely affects the chemical reaction rate. Since the inflow velocity of the electrolyte is kept constant, the lateral gas penetration is enhanced at higher current densities. Similar results have been observed in the experimental work of Riegel et al [3].

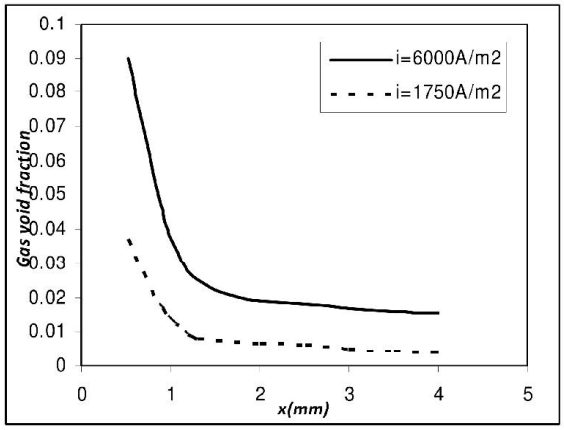

Fig. 4. Effect of current density on the gas release ($y=H/2$, $V_{in}=0.7m/s$).

The effect of the gap distance on the gas evolution is illustrated in Fig. 5 (W being the width of channel). In this case study, current density and inlet velocity of electrolyte are kept constant. It is seen that the void fraction decreases at the wider gap distances between the two electrodes. This may be attributed to the increased flow rate which swept formed gas easily at the larger gap distances. On the other hand, although void fraction decreases at a higher gap distance, the gas released in a time interval increases because of the higher flow rates.

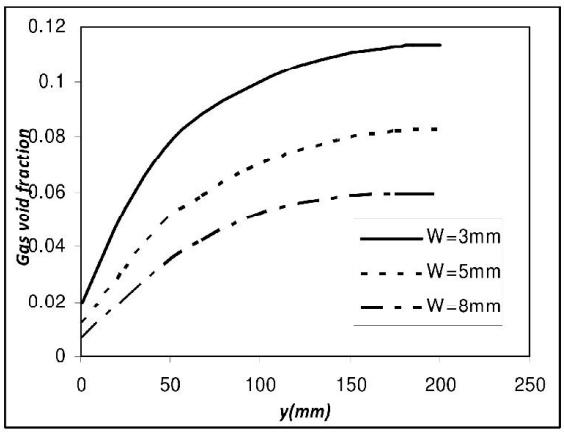

Fig. 5. Estimated gas void fraction distribution on the cathode at different cell gap distance along the electrode.

Fig.6 shows interfacial area profile predicted using Eq. (11). As shown, before formation of bubbles, interfacial area per unit volume is zero and then is increasing toward to the top of the channel because of buoyancy and convection of bubbles along the channel.

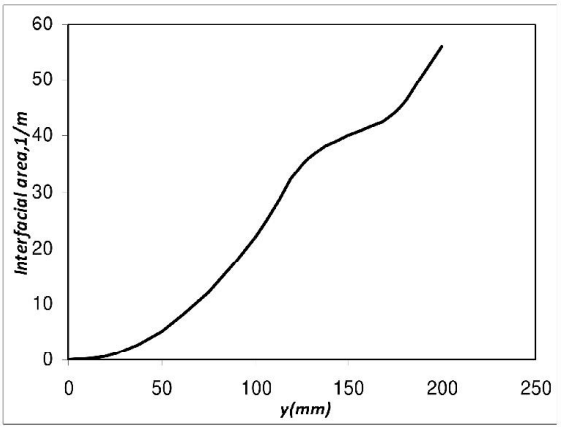

Fig. 6. Predicted interfacial area concentration along the channel.

Fig. 7 shows the distribution of bubble numbers per unit volume along the channel. The number of bubbles per unit volume N_b is calculated as:

$$N_b = \frac{6\alpha_g}{\pi d_b^3}, \tag{15}$$

It is seen that the bubble numbers is almost increases toward to the top of the channel. This observation suggests that the void growth in the downstream region of the channel is caused by bubble numbers increase, as demonstrated in Fig. 5.

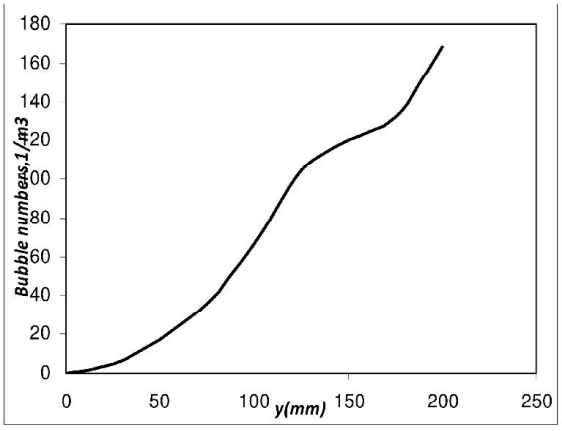

Fig. 7. Predicted distribution of bubble numbers along the channel.

CONCLUSION

Hydrogen gas evolution and void distribution in a vertical membrane electrochemical cell is investigated numerically using a two-phase flow model. The effect of current density, electrolyte flow rate and distance between electrodes on the gas

release rate are investigated in a range of parameter. It can be concluded that:

1) The predicted hydrogen void fraction increases along both the vertical and horizontal directions. The vertical increase is attributed to the accumulation of gas towards the top of the cell due to buoyancy, while the lateral increase is a result of the molecular diffusion.
2) It is found that the gas release rate increases as the electrolyte flow velocity increases due to the consequent decrease in the residence time of bubbles on the electrode.
3) The gas release rate was enhanced with higher applied current density; however, the increase is found to be not linear with the increase in current density due to the higher bubble content on the electrode surface diminishing the penetration of fresh electrolyte to reaction sites; thus, reducing the gas release rate.
4) For an efficient electrolysis process gas released should be removed from the reaction sites to increase surface areas available for the reaction.

REFERENCES

[1] Vogt H., Gas evolving electrodes, Comprehensive treatise of electrochemistry, *New York: Plenum Press, 1983, 6.*

[2] L. Muller, M. Krenz, K. Robner, on the relation between the transport of electrochemically evolved Cl_2, and H_2 into the electrolyte bulk by convective diffusion and by gas bubbles, *Electrochemical Acta, 1989, 34(3), 305-308.*

[3] Reigel H., Mitrovic J, Stephan K., Role of mass transfer on hydrogen evolution aqueous media, *Applied Electrochem., 1998, 28, 10–7.*

[4] Fukunaka Y., Kondo Y., Electrolyte circulation in electro-refining process, *Metal Rev MMIJ1, 1988, 5(1), 9–23.*

[5] Boissonneau P., Byrne P., an experimental investigation of hydrogen gas bubbles-induced free convection in small electrochemical cell, *Applied Electrochem., 2000,30, 767–75.*

[6] Hine F., Murakami K., Bubble effects on the solution IR drop in vertical electrolyzer under free and forced convection, Electrochem. *Soc., 1980, 127, 292–297.*

[7] Dahlkild A. A., Modeling the two-phase flow and current distribution along a vertical gas-evolving electrode, *Fluid Mech., 2001, 428, 249–72.*

[8] Mahmut D.Mat, Kemal Aldas, Application of a two-phase flow model for natural convection in an electrochemical cell, *International Journal of Hydrogen Energy, 2005, 30, 411 – 420.*

[9] Sherman C.P. Cheung, G.H. Yeoh, J.Y. Tu, On the modelling of population balance in isothermal vertical bubbly flows-Average bubble number density approach, *International journal of Chemical Engineering and Processing, 2007, 46, 742.*

[10] Thomas Nierhaus, David Vanden Abeele, Herman Deconinck, Direct numerical simulation of bubbly flow in the turbulent boundary layer of a horizontal parallel plate electrochemical reactor, *International Journal of Heat and Fluid Flow, 2007, 28, 1.*

[11] Jean St-Pierre, Anthony A. Wragg., Behavior of electro-generated and oxygen bubbles in narrow gap cells-part II application in chlorine production, *Electrochemical Acta, 1993, 38 (13), 1705-1710,*

[12] Jinsong Hua, Chi-Hwa Wang, Numerical Simulation of bubble-driven liquid flows, *International Journal of Chemical Engineering Science, 2000, 55, 4159-4173.*

[13] Simonin O. et al, Eulerian prediction of the fluid/particle correlated motion in turbulent two-phase flows, *Applied Scientific Research, 1993, 51, 275.*

[14] X. Li, R. Wang, R. Huang, Y. Shi, Numerical investigation of boiling flow of nitrogen in a vertical tube using the two-fluid model, *Applied Thermal Engineering, 2006, 26, 2425–2432.*

[15] Patankar S. V., Spalding D. B., A calculation procedure for heat, mass and momentum transfer in three-dimensional parabolic flows, *International Journal of Heat Mass Transfer, 1972, 15, 1787-1806.*